Cellulose (2020) 27:4963–4973
https://doi.org/10.1007/s10570-020-03125-6

ORIGINAL RESEARCH

Preparation and characterization of magnetic polyporous biochar for cellulase immobilization by physical adsorption

Haodao Mo · Jianhui Qiu · Chao Yang · Limin Zang · Eiichi Sakai

Received: 28 August 2019 / Accepted: 24 March 2020 / Published online: 7 April 2020

Abstract Because of the high specific surface area, polyporous structure and ease of preparation, porous biochar from lignocellulosic biomass is popular for being used as support for enzyme immobilization. In this work, polyporous biochar combined with magnetic particle γ-Fe_2O_3 was prepared by calcination and then used as support for cellulase adsorption. The effects of calcination temperature and time on the properties of magnetic polyporous biochar were investigated and the optimum preparation condition was obtained. For the cellulase adsorption, the immobilization capacity for the magnetic support reached as high as 266 mg/g with a relative activity of 73.6% compared with that of free cellulase. The behavior of cellulase adsorption showed that an endothermic process occurred more easily at high temperatures, which resulted in a high adsorption amount.

Keywords Polyporous biochar · Cellulase immobilization · Physical adsorption · Magnetism

H. Mo · J. Qiu (✉) · E. Sakai
Department of Machine Intelligence and Systems Engineering, Faculty of Systems Engineering, Akita Prefectural University, 84-4 Aza Ebinokuchi Tsuchiya, Yurihonjo City, Akita 015-0055, Japan
e-mail: qiu@akita-pu.ac.jp

C. Yang · L. Zang
College of Materials Science and Engineering, Guilin University of Technology, Guilin, China

Introduction

In recent years, new sustainable energy, especially bioethanol, has received wide attention. As a "green" approach, preparation of bioethanol from lignocellulosic biomass by enzymatic hydrolysis and biofermentation is very popular, due to the environmental friendly and low production cost (Sassner et al. 2008; Haghighi et al. 2013). Cellulase is a kind of complex enzyme, which consists of endoglucanase, exoglucanase and β-glucosidase. It is very useful in the lignocellulosic cellulose hydrolysis for glucose production (Bansal et al. 2009; Chander et al. 2016; Lin et al. 2017). However, cellulase has good water solubility, which makes it difficult to separate from the products and cannot be recycled. Therefore, effective recovery and reuse of cellulase has received great attention.

Immobilization of bioactive materials such as DNA (Ramakrishnan et al. 2016), protein (Rusmini et al. 2007), enzyme (Altinkaynak et al. 2016) and cell (Kumar et al. 2016) on the surface of solid has been proven to be effective and feasible to recover and improve the stability and reusability of the bioactive materials. In general, the immobilization methods can be divided into physical adsorption and covalent bonding. Physical adsorption includes van der Waals force, ionic bonds, and the hydrogen bonds between solid materials and enzymes (Zang et al. 2014). Covalent bonding means that the activated functional groups of support react with other groups (–COOH, –

NH_2, –SH, etc.) (Barbosa et al. 2013) on the surface of the enzyme to produce covalent bonds, thereby binding the enzyme onto the support.

For the physical method, it is convenient and rarely changes the structure of enzyme, thus retaining most of the enzyme's activity (Teofil et al. 2014). Mesoporous materials have a large specific surface area, a variety of pore structures and high biocompatibility (Zhou 2013), which are desirable supports for enzyme immobilization. Piras (Piras et al. 2011) prepared immobilized human lysozyme loaded into the pores of SBA-15 mesoporous silica by the immunogold staining method. Bhattacharyya (Bhattacharyya et al. 2010) studied two ordered mesoporous materials that presented similar structure and texture but had different chemical composition and surface properties for lysozyme adsorption. The adsorbents showed a high lysozyme adsorption amount and provided a crucial size-selective parameter to address guest enzyme adsorption. However, for the mesoporous materials, especially silica mesoporous materials with order pore structure, how to design the size of the pore would directly affect the adsorption amount of enzyme. Simultaneously, the microenvironment of the inner of pore and the surface of adsorbent are quite different, and the mobility and flexibility of enzyme would be limited more inside the pore. Furthermore, the enzyme inside the pore is difficult or even impossible to participate in the hydrolysis reaction (Yuichi et al. 2014). Therefore, developing adsorbents with large specific area, open pore structure and plenty attachment points on the surface for enzyme immobilization may relieve these negative effects.

Polyporous biochar is a kind of solid material formed from the thermochemical decomposition of lignocellulosic materials (Ahmad et al. 2014; Cha et al. 2016). The main element components of biochar contain carbon, oxygen and hydrogen, and it is usually used in wastewater treatment (Thompson et al. 2016) and electrode material (Qian et al. 2015). However, the polyporous biochar-based adsorbent for cellulase adsorption has been rarely reported. On the one hand, polyporous biochar with high specific surface area and rich pore structure can provide more active sites for enzyme immobilization. On the other hand, polyporous biochar has a wide range of sources, which means it is easy to be obtained and economical. Thus, it could be an ideal adsorbent for cellulase adsorption. In addition, to facilitate recycling, combining with magnetic materials could allow selective recovering from the reaction medium by applying an external magnetic field. However, there are few literatures on the preparation of magnetic polyporous biochar by calcination method that could generate a uniform magnetic particles on the surface of polyporous biochar. With the assistance of calcination method, the magnetic polyporous biochar for cellulase immobilization could be expected.

Therefore, in this work, for the adsorbent preparation, the magnetic polyporous biochar was prepared by calcination method, where the calcination time and temperature have been considered. For the cellulase adsorption, the structure of adsorbent, adsorption temperature and the adding amount of adsorbent were considered for the discussion of cellulase adsorption behavior. Finally, there was a simple evaluation of the enzymatic and reusability of the immobilized enzyme.

Experimental

Materials

Sugarcane bagasse was collected from Guangxi, China. Potassium hydroxide (KOH), hydrochloric acid (HCl, 35–37wt %), ferric chloride hexahydrate ($FeCl_3{\cdot}6H_2O$), ferrous chloride tetrahydrate ($FeCl_2{\cdot}4H_2O$), ethanol and carboxyl methyl cellulose sodium (CMC) were purchased from Nacalai Tesque, Inc. (Tokyo, Japan). Cellulase was bought from Meiji Seika Pharma Co., Ltd (Tokyo, Japan).

Preparation of polyporous biochar

The pyrolysis process for the preparation of porous biochar is widely reported, and the biomass material is usually activated by KOH (Azargohar and Dalai 2008) to obtain a larger specific surface area. Bagasse was pulverized (< 1 mm) and boiled in water at 95 °C for 8 h. After being dried at 60 °C for 24 h, the bagasse was mixed with KOH and ethanol (1 g:1 g:12 mL) in a beaker at 60 °C for 5 h, and the mixture was dried at 60 °C for 12 h. Then, the dried mixture was put in a tube furnace and carbonized at 800 °C for 2 h under a N_2 protection and with a heating rate of 10 °C/min. The generated products were ground and immersed in 12.5 mL of 1.5 M HCl for 2 h to remove the ash and alkali. After being washed with distilled water several

times and dried at 60 °C for 24 h, the polyporous biochar was obtained and denoted as C.

Preparation of magnetic polyporous biochar (C/γ-Fe_2O_3)

In order to better combine C and γ-Fe_2O_3, a calcination method has been used. At the same time, the temperature and time of calcination as well as the ratio of C, Fe^{3+} and Fe^{2+} were discussed. (a) Calcination temperature: 0.1 g C was added in 2 mL ethanol solution (containing 0.2 mmol $FeCl_3{\cdot}6H_2O$ and 0.1 mmol $FeCl_2{\cdot}4H_2O$). The mixture was dried at 70 °C for 10 min in tube furnace, and then the temperature was raised to 400–700 °C and kept for 1 h (N_2 protection, heating rate of 10 °C/min). (b) Calcination time: the experimental procedure was similar as mentioned above. The calcination temperature was 500 °C and the calcination time was set from 10 to 120 min. (c) The ratio of C, Fe^{2+} and Fe^{3+}: the mixture of C, $FeCl_3{\cdot}6H_2O$ and $FeCl_2{\cdot}4H_2O$ with three ratios of 0.1 g:0.2 mmol:0.1 mmol, 0.1 g:0.4 mmol:2 mmol, and 0.1 g:1 mmol:0.5 mmol were calcined at 500 °C for 1 h, respectively. The specific conditions are listed in Table 1.

Immobilization of cellulase

A certain amount of support was added in 10 mL cellulase solution (pH 4). The solution was placed into an air bath shaker and shaken with an oscillation speed of 120 r/min for 12 h. During this process, 0.2 mL mixture was taken out. After separation by magnet, 0.05 mL supernatant was used for the determination of residual cellulase concentration at 30 min, 1 h, 3 h, 6 h, 9 h and 12 h, respectively. The residual concentration of cellulase was determined by the Bradford protein assay method and the cellulase loading amount was calculated from the following equation:

$$\text{Immobilized amount} = C_0V_0 - C_1V_1$$

where C_0 and V_0 is the concentration and volume of initial cellulase solution, respectively. The C_1 and V_1 is the concentration and volume of cellulase solution after immobilization, respectively.

Characterization

The structure and composition of samples were characterized by the X-ray diffraction (XRD) using a PANalytical X' Pert Pro (UK) instrument. The magnetism of C/γ-Fe_2O_3 was determined by vibrating-sample (VSM, Riken Denshi Co. Ltd., Japan). The specific surface areas of samples were determined by Brunauer–Emmett–Teller (BET) nitrogen adsorption method at 77 K using ASAP 2020 analyzer (Micromeritics, USA). The morphologies of samples were analyzed by scanning electron microscope (SEM, Hitachi S-4300, Japan). The cellulase concentrations were determined by UV–Vis spectrophotometer (UV–Vis, U-5100, Japan).

Table 1 Preparation conditions of C/γ-Fe_2O_3

Number	C (g)	$FeCl_2{\cdot}4H_2O$ (mmol)	$FeCl_3{\cdot}6H_2O$ (mmol)	Temperature (°C)	Time (min)	Remarks
Temperature variable	0.1	0.1	0.2	400	60	
	0.1	0.1	0.2	500	60	
	0.1	0.1	0.2	600	60	
	0.1	0.1	0.2	700	60	
Time variable	0.1	0.1	0.2	500	10	
	0.1	0.1	0.2	500	30	
	0.1	0.1	0.2	500	60	
	0.1	0.1	0.2	500	90	
	0.1	0.1	0.2	500	120	
Feeding ratio variable	0.1	0.1	0.2	500	60	1#
	0.1	0.2	0.4	500	60	2#
	0.1	0.5	1	500	60	3#

Activity assay

The cellulase activity was evaluated according to IUPAC method (Ghose 1987). An immobilized cellulase containing 0.2 mg of cellulase was added in 10 mL 1% CMC solution (pH 4). After being hydrolysed at 50 °C for 30 min, the mixture was separated by a magnet for 5 min. Then, 1 mL supernatant was mixed with 2 mL DNS solution. The mixing solution was put into boiling water for 5 min. Finally, 10 mL distilled water was added to dilute the reaction solution. The amount of glucose was determined by a UV–Vis spectrophotometer at 540 nm. The International Unit of cellulase activity (IU/mg cellulase) is defined as a certain amount of cellulase that hydrolyzes CMC to produce 1 μmol glucose per minute.

Reusability assay

For an application factor, a long enzymatic hydrolysis time would be a good method to determine the reusability of immobilized enzyme (Zang et al. 2014). The immobilized cellulase (containing 3 mg cellulase) was distributed in 10 mL 1% CMC solution (pH 4) for 24 h of hydrolysis at 50 °C. After separation by a magnet, the mass of glucose in supernatant was determined by UV–Vis spectrophotometer at 540 nm, and the immobilized enzyme was added into a fresh substrate solution for a new hydrolysis. This process was repeated 5 times.

$$\text{The recovery rate} = M_n/M_1 \times 100\%$$

where M_n is the mass of glucose produced by the nth saccharification, and the M_1 is mass of glucose produced at the first time.

Results and discussions

Characterizations of C/γ-Fe_2O_3 composites

The SEM images of C and C/γ-Fe_2O_3 composites are given in Figs. 1 and 2. From the SEM image of C (Fig. 1a), a clearly allium-giganteum-like porous structure (Chen et al. 2017b) is found, and it has a smooth surface. After calcination, a lot of crystals grow on the surface of C/γ-Fe_2O_3 composites, indicating that γ-Fe_2O_3 has grown well on the surface of porous biochar (Fig. 1b–e). In Fig. 1, the calcination temperature shows an important influence on the formation of γ-Fe_2O_3. At first, only some needle crystals are formed at 400 °C (Fig. 1b). As the temperature increases, the amount of crystallization also increases (Fig. 1c, d). However, when the temperature further reaches 700 °C, the amount of crystallization is reduced (Fig. 1e), which means that excessive temperature would destroy the structure of γ-Fe_2O_3. The effect of calcination time on the formation of crystals can be visually seen from Fig. 2, which is similar to the effect of calcination temperature. At the calcination time of 60 and 90 min, the crystals are well distributed in the polyporous biochar surface and the macroporous. However, as shown in Fig. 2e, a long time could reduce the amount of crystallization.

The calcination temperature and time have great influence on the formation of magnetic particles. The XRD patterns of C and C/γ-Fe_2O_3 composites with different calcination temperature are shown in Fig. 3a. For polyporous biochar, a broad diffraction peak appears at 23.1°, which is attributed to the (002) plane of graphite resulted from its amorphous nature. Meanwhile, the (100) plane of graphite is found at 43.4° (a weak diffraction peak) (Chen et al. 2017c). The results prove that bagasse has been completely converted after pyrolysis. For C/γ-Fe_2O_3 composites calcined at 500 °C, there are 9 diffraction peaks at 2θ = 18.3°, 25.0°, 30.0°, 35.4°, 37.0°, 43.0°, 53.4°, 56.9° and 62.5°, which are assigned to the diffraction of (111), (210), (220), (311), (222), (400), (422), (511) and (400) planes of γ-Fe_2O_3 (JCPDS card No. 39-1346) (Wu et al. 2015), respectively. When the temperature is higher than 500 °C, some diffraction peaks of γ-Fe_2O_3 become weak or even disappear because the high temperature would give rise to the partial transformation of magnetic hematite into hematite (Monte et al. 1997). Figure 3b shows the XRD patterns of C/γ-Fe_2O_3 composites with different calcination time. The diffraction peaks of γ-Fe_2O_3 can be clearly found when the calcination time is 1 h. The results show that a shorter calcination time is not conducive to the formation of γ-Fe_2O_3, while a longer calcination time would destroy the structure of γ-Fe_2O_3 at 500 °C. Thus, 500 °C and 1 h are the optimum calcination conditions for the C/γ-Fe_2O_3 composites.

The magnetization curves for C/γ-Fe_2O_3 composites at room temperature are shown in Fig. 4. The

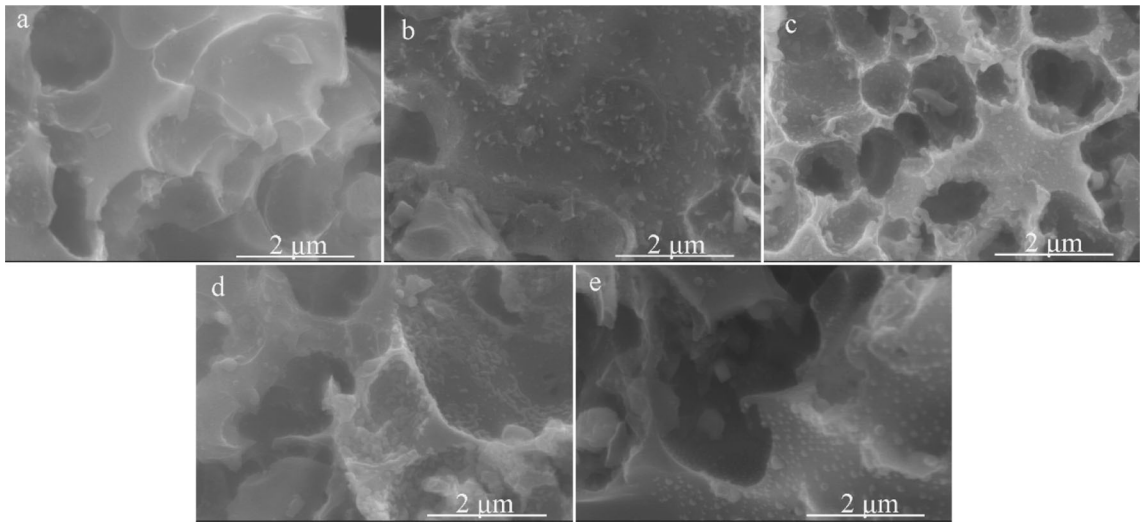

Fig. 1 SEM images of **a** C and C/γ-Fe_2O_3 composites calcined at **b** 400 °C, **c** 500 °C, **d** 600 °C and **e** 700 °C for 1 h

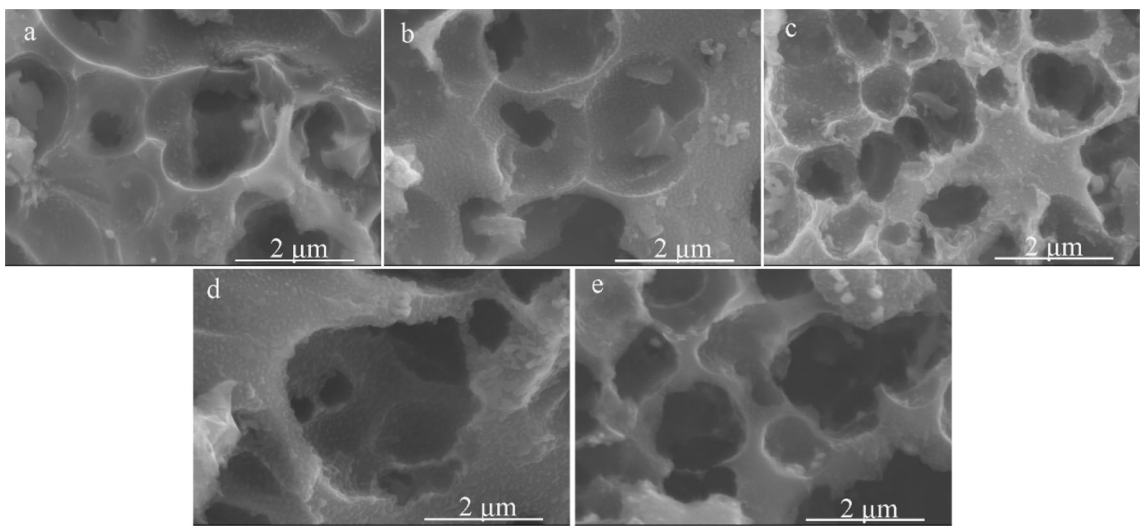

Fig. 2 SEM images of C/γ-Fe_2O_3 composites calcined at 500 °C for **a** 10 min, **b** 30 min, **c** 60 min, **d** 90 min and **e** 120 min

results show that the C/γ-Fe_2O_3 composites calcined at 500 °C for 1 h has the highest saturation magnetization of 0.51 emu/g. Only a small amount of γ-Fe_2O_3 is formed with low calcination temperature and short calcination time. However, with high calcination temperature or long calcination time, the magnetic hematite would be converted into hematite. The results are consistent with the results from SEM and XRD.

Immobilization of cellulase by C/γ-Fe_2O_3 composites

Considering the morphology and saturation magnetization, the C/γ-Fe_2O_3 composites calcined at 500 °C for 1 h were chosen as support for cellulase adsorption. For the enzyme adsorption, the effects of adsorption temperature and amount of adsorbent were studied (Hudson et al. 2008).

To investigate the effect of the ratio of C, Fe^{2+} and Fe^{3+} on cellulase adsorption, 50 mg C/γ-Fe_2O_3 composites was added in 10 mL 4 mg/mL cellulase

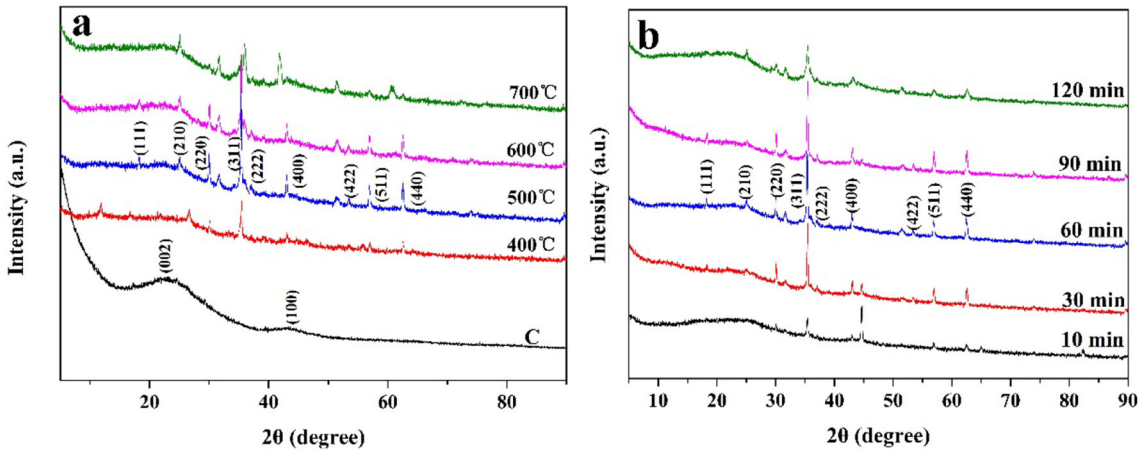

Fig. 3 X-ray diffraction patterns for C and C/γ-Fe_2O_3 composites with different calcination temperature (**a**) and time (**b**)

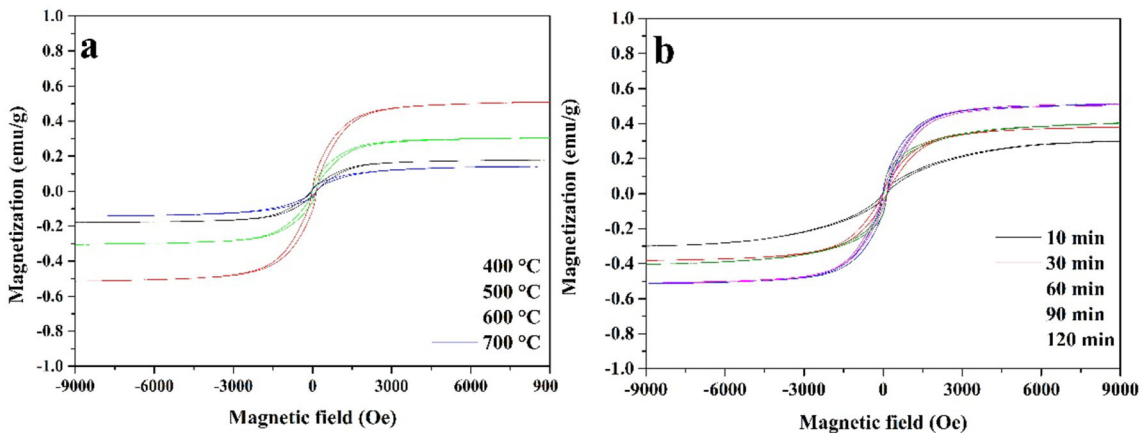

Fig. 4 Magnetization curves for C/γ-Fe_2O_3 composites with different calcination temperature (**a**) and time (**b**)

solution with an air bath oscillator at 50 °C for 12 h. Figure 5 illustrates that 1#, 2# and 3# have similar adsorption curves. After adsorption for 30 min, the cellulase adsorption amount of 1#, 2# and 3# reach 108, 118 and 96 mg/g respectively, indicating that C/γ-Fe_2O_3 composites have good adsorption ability for cellulase. In addition, there are slight difference of their adsorption curve after 9 h. 1#, 2# and 3# are close to a state of balance, while they are still slowly rising. It should be further explained in conjunction with the structure of C/γ-Fe_2O_3 composites.

As the ratio of C, Fe^{2+} and Fe^{3+} increases, the amount of crystallization also increases. The morphology of the polyporous biochar changed significantly. Especially for 3#, there is a stack of γ-Fe_2O_3 on the surface of polyporous biochar (Fig. 6). Meanwhile, the highest saturation magnetization increased from 0.51 to 1.74 emu/g (Fig. 7b). However, the X-ray diffraction patterns of 1#, 2# and 3# indicate that their crystallization structure has not been changed (Fig. 7a). All the composites show a combined I/IV sorption isotherm in the N_2 adsorption–desorption isotherm (Fig. 8), which indicates that there is a composite pore structure in the C/γ-Fe_2O_3 composites (Chen et al. 2017b). The pore size, BET surface area, total pore volume, cellulase adsorption amount and zeta potential are given in Table 2. Compared with 1# and 2#, the BET surface area of 3# is less than half. It is obviously caused by that the γ-Fe_2O_3 is deposited on the surface of the polyporous biochar as well as in the pores (Fig. 6). However, the cellulase adsorption amount of 1#, 2# and 3# are not much different, which are 266, 260, 252 mg cellulase/g adsorbent after adsorption for 12 h, respectively.

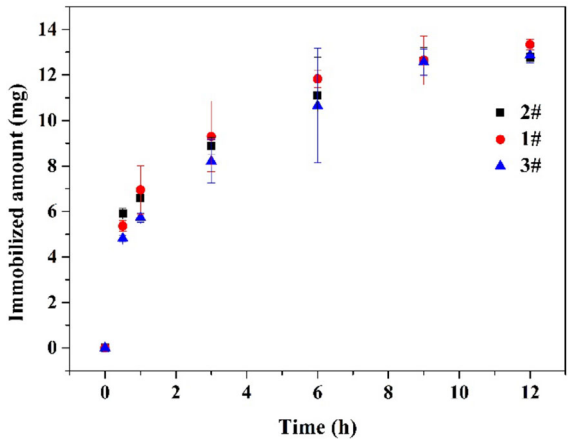

Fig. 5 Different adsorbents for cellulase adsorption (adsorption condition: 50 mg C/γ-Fe_2O_3 composites and 10 mL 4 mg/mL cellulase solution with an air bath oscillator at 50 °C for 12 h)

This should be due to the size of the pore and cellulase. Cellulase is an elongated object, and the horizontal and vertical are 12.4 and 3.7 nm (Chen et al. 2017a), which is bigger than the average pore size of the adsorbents. Thus, many mesoporous structures inside the adsorbent cannot accommodate one cellulase molecule. The cellulase should be adsorbed on the surface of C/γ-Fe_2O_3 composites. Simultaneously, the zeta potentials of 1#, 2# and 3# are − 37.94 ± 5.35, − 21.28 ± 6.44 and 30.39 ± 6.08 mV, respectively. This shows that all three materials have strong adsorption capacity. Eventually, the adsorption amounts of the three adsorbents are not much different. However, there is still a part of cellulase that is immobilized by pore adsorption, but the process is slow. Thus, after 12 h of adsorption, the cellulase adsorption amount still rises slowly.

50 mg of 1# was added in 10 mL 4 mg/mL cellulase solution with an air bath oscillator for 12 h at 20, 35 and 50 °C, respectively. As given in Fig. 9, with the increasing temperature, the adsorption amount of cellulase is increased in the whole temperature range. According to the above analysis, a part of cellulase is adsorbed by pore adsorption. At a higher temperature, it is easy to break the initial interaction between the protein and the adsorbent surface and

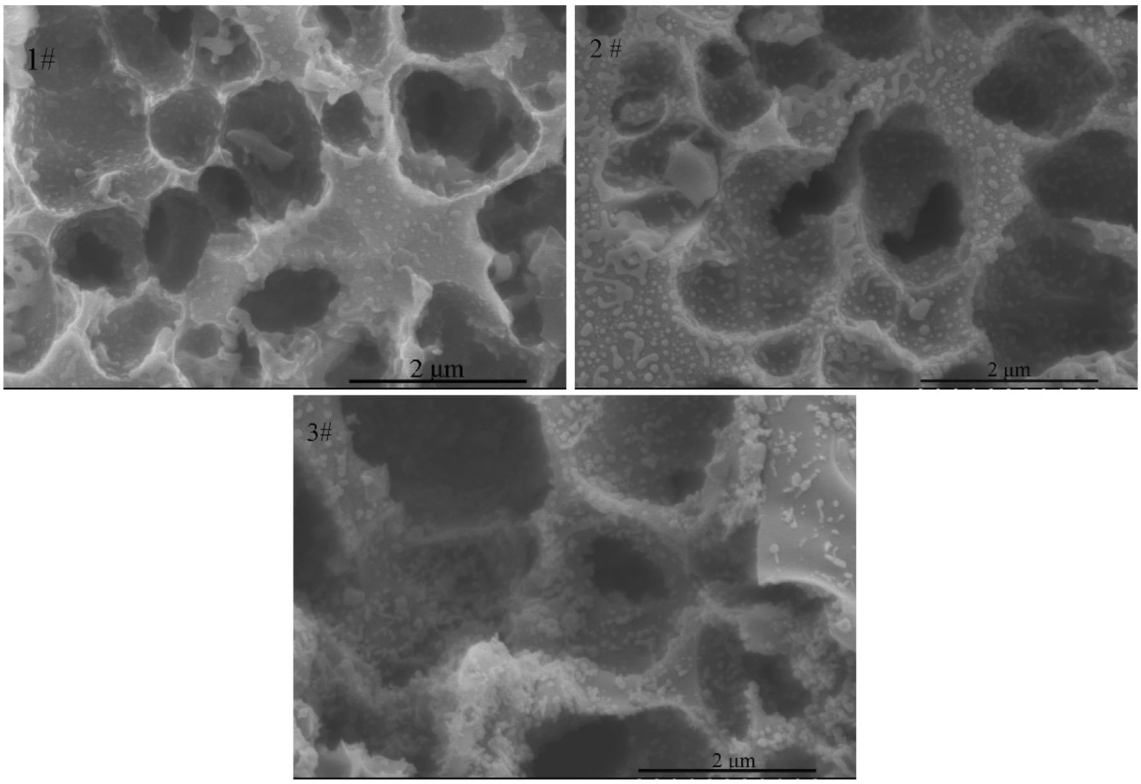

Fig. 6 The SEM images of 1#, 2# and 3#

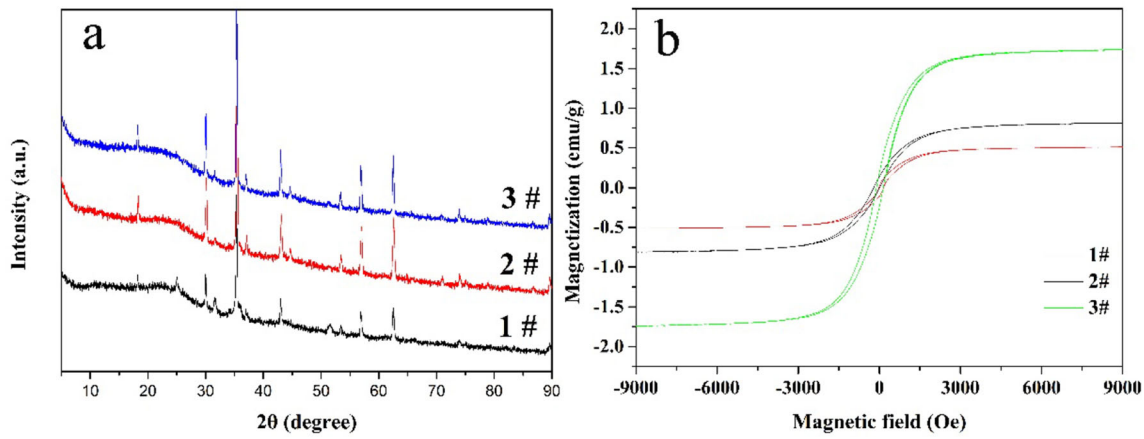

Fig. 7 The XRD patterns (**a**) and magnetization curves (**b**) of 1#, 2# and 3#

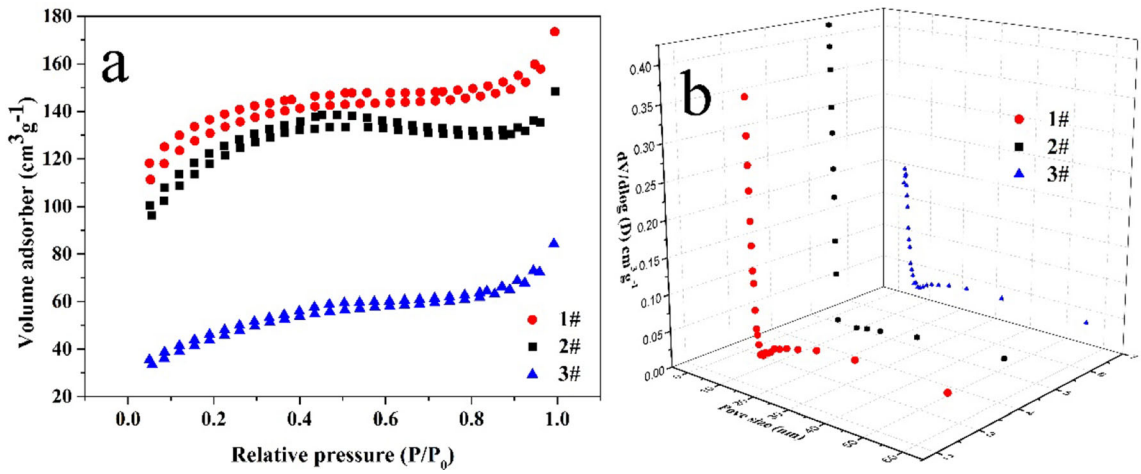

Fig. 8 N_2 adsorption–desorption isotherm (**a**) and the pore size distribution (**b**) by BJH method of different C/γ-Fe_2O_3 composites

Table 2 The average pore size, BET surface area, total pore volume, cellulase adsorption amount and zeta potential of C/γ-Fe_2O_3 composites

C/γ-Fe_2O_3 composites	Average pore size (nm)	BET surface area (m^2/g)	Total pore volume ($cm^{3/g}$)	Adsorbed amount (mg/g)	Zeta potential (mV)
1#	3.6	422.6	0.119	266	− 37.94 ± 5.35
2#	3.3	393.9	0.113	260	− 21.28 ± 6.44
3#	2.7	156.5	0.103	252	30.39 ± 6.08

occurs an endothermic process (Lei et al. 2004). Thus, the adsorption amount of cellulase would increase when the temperature increases. However, considering excessive temperature that can cause enzyme inactivation, 50 °C is determined as the optimum adsorption temperature in this work.

At a certain enzyme concentration, the amount of adsorbent has a direct effect on the amount of enzyme adsorption. As shown in Fig. 10, 10, 50 and 100 mg of 1# were added in 10 mL 4 mg/mL cellulase solution with an air bath oscillator for 12 h at 50 °C. Obviously, the total amount of adsorption increases

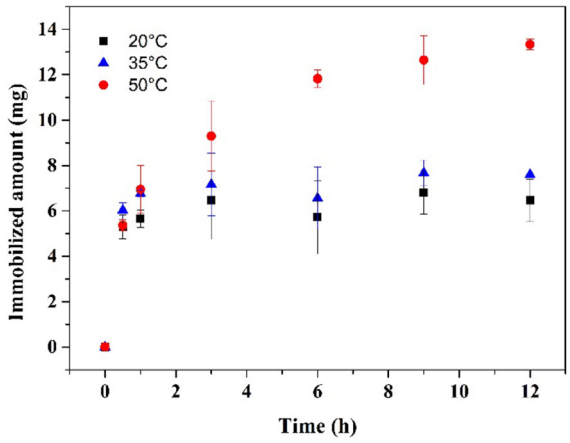

Fig. 9 Different temperature for cellulase adsorption (adsorption condition: 50 mg C/γ-Fe_2O_3 composites and 10 mL 4 mg/mL cellulase solution with an air bath oscillator for 12 h at 20, 35 and 50 °C, respectively)

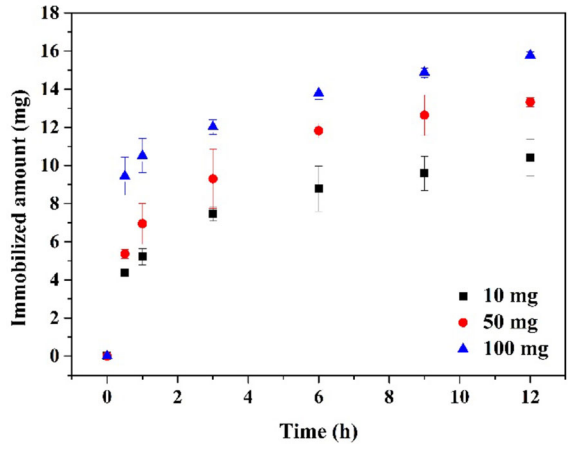

Fig. 10 Different adsorbent amount for cellulase adsorption (adsorption condition: 10, 50 and 100 mg C/γ-Fe_2O_3 composites and 10 mL 4 mg/mL cellulase solution with an air bath oscillator for 12 h at 50 °C, respectively)

as the amount of adsorbent increases, and the adsorption rate of cellulase are 26.0%, 33.3% and 39.5%, respectively. When the unit is converted to mg cellulase/g adsorbent, the enzyme loading amount is 1040, 266 and 158 mg cellulase/g adsorbent, respectively. However, it can be predicted that when the adsorbent is added in an amount of 10 mg, the cellulase on the surface of the composite may be stacked. Therefore, 50 mg adding adsorbent should be the optimum adding amount in this work.

Compared with some recently reported literature (Table 3), the magnetic polyporous biochar possessed excellent performances for cellulase adsorption. This should be attributed to the magnetic polyporous biochar has a high specific surface area, rich pore structure and a high zeta potential which can provide more sites for enzyme immobilization. In addition, this kind of magnetic polyporous biochar is easily obtained and widely available. Therefore, the magnetic polyporous biochar prepared in this work is considered to have practical value.

Activity assays

The structure or microenvironment of the cellulase was changed after being adsorbed to the surface of adsorbent, which would change the activity of the enzyme. Figure 11 shows the relative activity of free cellulase, 1#, 2# and 3# immobilized cellulase. Compared with that of free cellulase, the relative activity of 1#, 2# and 3# immobilized cellulase is 73.6%, 66.0% and 57.5%, respectively. The mobility and flexibility of immobilized cellulase would weaken when it is immobilized onto the surface of adsorbent, leading to a decrease in the activity of cellulase.

Reusability assays

To compare the relative activity of 1#, 2# and 3#, 1# was selected for reusability assays. As shown in Fig. 12, after the hydrolysis of CMC by 1# for 24 h, the glucose yield is 259.3 mg glucose/g CMC. However, as the number of uses increases, the glucose yield gradually decreases. This may be caused by the following reasons. The physical adsorption may be not strong enough, and the cellulase desorbs from the surface of polyporous biochar during the hydrolysis process. In addition, the end-product inhibition and protein denaturation may also cause the loss of activity of the immobilized cellulase (Jordan et al. 2011).

Conclusions

In this work, calcination method was used for the preparation of magnetic polyporous biochar. Calcination temperature and time show direct impacts on the formation of C/γ-Fe_2O_3. As the temperature increases, the amount of crystallization increases. However, higher temperature or long-term calcination would destroy the structure of γ-Fe_2O_3. The optimum

Table 3 Adsorbent, adsorbate, adsorption time and capacity of the current work and other reports

Adsorbent	Adsorbate	Adsorption time (h)	Adsorption capacity (mg/g)	References
PS-DVB-g-PS-g-PANI	Cellulase	2	7.2	Ince et al. (2012)
MNPs-APTES-Cu	Cellulase	3	164	Abbaszadeh and Hejazi (2019)
PAA nanogel	Cellulase	2	87.3	Ahmed et al. (2017)
Mesoporous silica	Cellulase	24	271.7	Chen et al. (2017a)
PVA-co-PE NFM	cellulase	4	130	Amaly et al. (2018)
Magnetic polyporous biochar	Cellulase	12	266	The current work

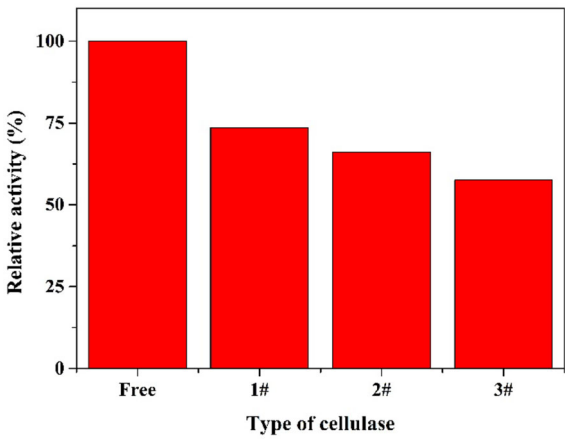

Fig. 11 The relative activity of types of cellulase (reaction condition: an immobilized cellulase containing 0.2 mg of cellulase and 10 mL 1% CMC solution (pH 4) with an air bath oscillator for 30 min at 50 °C)

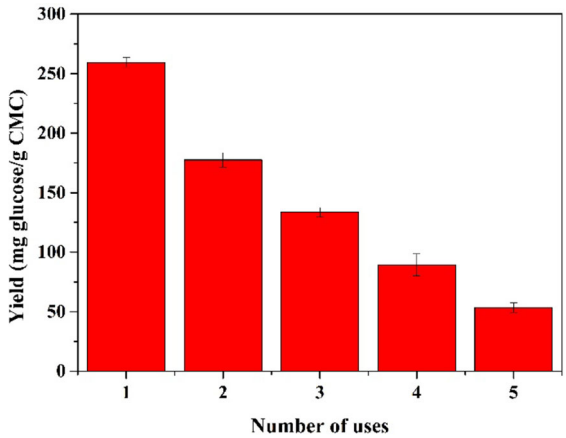

Fig. 12 The effect of recycles on the glucose productivity of immobilized cellulase (reaction condition: an immobilized cellulase containing 3 mg of cellulase and 10 mL 1% CMC solution (pH 4) with an air bath oscillator for 24 h at 50 °C)

condition is confirmed: calcination temperature is 500 °C and calcination time is 60 min. The large specific surface area (422.6 m^2/g) of 1# has a high zeta potential (− 37.94 ± 5.35 mV), which shows a good cellulase adsorption capacity (266 mg cellulase/g adsorbent) after 12 h of adsorption at 50 °C. Simultaneously, the immobilized cellulase retains 73.6% of the activity compared with free cellulase (at 50 °C and pH 4). Besides, it has some reusability which maintains 51.7% glucose yield after three uses.

Acknowledgments We thank associate Prof. Komiyama for the help of VEM test and Dr. Wang for the help of BET test in this study.

References

Abbaszadeh M, Hejazi P (2019) Metal affinity immobilization of cellulase on Fe_3O_4 nanoparticles with copper as ligand for biocatalytic applications. Food Chem 290:47–55. https://doi.org/10.1016/j.foodchem.2019.03.117

Ahmad M, Upamali A, Eun J et al (2014) Biochar as a sorbent for contaminant management in soil and water: a review. Chemosphere 99:19–33. https://doi.org/10.1016/j.chemosphere.2013.10.071

Ahmed IN, Chang R, Tsai WB (2017) Poly(acrylic acid) nanogel as a substrate for cellulase immobilization for hydrolysis of cellulose. Colloids Surf B 152:339–343. https://doi.org/10.1016/j.colsurfb.2017.01.040

Altinkaynak C, Tavlasoglu S, Özdemir N, Ocsoy I (2016) A new generation approach in enzyme immobilization: organic-inorganic hybrid nanoflowers with enhanced catalytic activity and stability. Enzyme Microb Technol 93–94:105–112. https://doi.org/10.1016/j.enzmictec.2016.06.011

Amaly N, Si Y, Chen Y et al (2018) Reusable anionic sulfonate functionalized nanofibrous membranes for cellulase enzyme adsorption and separation. Colloids Surf B 170:588–595. https://doi.org/10.1016/j.colsurfb.2018.06.019

Azargohar R, Dalai AK (2008) Steam and KOH activation of biochar: experimental and modeling studies. Microporous

Mesoporous Mater 110:413–421. https://doi.org/10.1016/j.micromeso.2007.06.047

Bansal P, Hall M, Realff MJ et al (2009) Modeling cellulase kinetics on lignocellulosic substrates. Biotechnol Adv 27:833–848. https://doi.org/10.1016/j.biotechadv.2009.06.005

Barbosa O, Torres R, Ortiz C et al (2013) Heterofunctional supports in enzyme immobilization: from traditional immobilization protocols to opportunities in tuning enzyme properties. Biomacromol 14:2433–2462. https://doi.org/10.1021/bm400762h

Bhattacharyya MS, Hiwale P, Piras M et al (2010) Lysozyme Adsorption and Release from Ordered Mesoporous Materials. J Phys Chem C 114:19928–19934

Cha JS, Park SH, Jung S et al (2016) Production and Utilization of Biochar: a Review. J Ind Eng Chem 40:1–15. https://doi.org/10.1016/j.jiec.2016.06.002

Chander R, Deswal D, Sharma S et al (2016) Revisiting cellulase production and rede fi ning current strategies based on major challenges. Renew Sustain Energy Rev 55:249–272. https://doi.org/10.1016/j.rser.2015.10.132

Chen B, Qiu J, Mo H et al (2017a) Synthesis of mesoporous silica with different pore sizes for cellulase immobilization: pure physical adsorption. New J Chem 41:9338–9345. https://doi.org/10.1039/c7nj00441a

Chen J, Qiu J, Wang B et al (2017b) Manganese dioxide/biocarbon composites with superior performance in supercapacitors. J Electroanal Chem 791:159–166. https://doi.org/10.1016/j.jelechem.2017.03.025

Chen J, Qiu J, Wang B et al (2017c) Fe_3O_4/biocarbon composites with superior performance in supercapacitors. J Electroanal Chem 804:232–239. https://doi.org/10.1016/j.jelechem.2017.09.028

Ghose TK (1987) Measurement of cellulase activities. Pure Appl Chem. https://doi.org/10.1351/pac198759020257

Haghighi S, Hossein A, Tabatabaei M (2013) Lignocellulosic biomass to bioethanol, a comprehensive review with a focus on pretreatment. Renew Sustain Energy Rev 27:77–93. https://doi.org/10.1016/j.rser.2013.06.033

Hudson S, Cooney J, Magner E (2008) Proteins in mesoporous silicates. Angew chemie Int Ed 47:8582–8594. https://doi.org/10.1002/anie.200705238

Ince A, Bayramoglu G, Karagoz B et al (2012) A method for fabrication of polyaniline coated polymer microspheres and its application for cellulase immobilization. Chem Eng J 189–190:404–412. https://doi.org/10.1016/j.cej.2012.02.048

Jordan J, Kumar CSSR, Theegala C (2011) Preparation and characterization of cellulase-bound magnetite nanoparticles. J Mol Catal B Enzym 68:139–146. https://doi.org/10.1016/j.molcatb.2010.09.010

Kumar G, Mudhoo A, Sivagurunathan P, Nagarajan D (2016) Recent insights into the cell immobilization technology applied for dark fermentative hydrogen production. Bioresour Technol 219:725–737. https://doi.org/10.1016/j.biortech.2016.08.065

Lei J, Fan J, Yu C et al (2004) Immobilization of enzymes in mesoporous materials: controlling the entrance to nanospace. Microporous Mesoporous Mater 73:121–128. https://doi.org/10.1016/j.micromeso.2004.05.004

Lin Y, Liu X, Xing Z et al (2017) Preparation and characterization of magnetic Fe_3O_4—chitosan nanoparticles for cellulase immobilization. Cellulose 24:5541–5550. https://doi.org/10.1007/s10570-017-1520-6

Monte F, Morales MP, Levy D et al (1997) Formation of γ-Fe_2O_3 isolated nanoparticles in a silica matrix. Langmuir 7463:3627–3634

Piras M, Salis A, Piludu M, Monduzzi M (2011) 3D vision of human lysozyme adsorbed onto a SBA-15 nanostructured matrixw. Chem Commun 47:7338–7340. https://doi.org/10.1039/c1cc11840d

Qian K, Kumar A, Zhang H et al (2015) Recent advances in utilization of biochar. Renew Sustain Energy Rev 42:1055–1064. https://doi.org/10.1016/j.rser.2014.10.074

Ramakrishnan S, Krainer G, Grundmeier G et al (2016) Structural stability of DNA origami nanostructures in the presence of chaotropic agents. Nanoscale 8:10398–10405. https://doi.org/10.1039/c6nr00835f

Rusmini F, Zhong Z, Feijen J (2007) Protein immobilization strategies for protein biochips. Biomacromol 8:1775–1789

Sassner P, Galbe M, Zacchi G (2008) Techno-economic evaluation of bioethanol production from three different lignocellulosic materials. Biomass Bioenergy 32:422–430. https://doi.org/10.1016/j.biombioe.2007.10.014

Teofil J, Jakub Z, Krajewska B (2014) Enzyme immobilization by adsorption: a review. Adsorption. https://doi.org/10.1007/s10450-014-9623-y

Thompson KA, Shimabuku KK, Kearns JP et al (2016) Environmental comparison of biochar and activated carbon for tertiary wastewater treatment. Environ Sci Technol 50:11253–11262

Wu H, Wu G, Wang L (2015) Peculiar porous α-Fe_2O_3, γ-Fe_2O_3 and Fe_3O_4 nanospheres: facile synthesis and electromagnetic properties. Powder Technol 269:443–451. https://doi.org/10.1016/j.powtec.2014.09.045

Yuichi M, Shin-ichi K, Yuki K, Katsuya K (2014) Interparticle mesoporous silica as an effective support for enzyme immobilisation. RSC Adv 4:3573–3580. https://doi.org/10.1039/c3ra46122j

Zang L, Qiu J, Wu X et al (2014) Preparation of magnetic chitosan nanoparticles as support for cellulase immobilization. Ind Eng Chem Res 53:3448–3454. https://doi.org/10.1021/ie404072s

Zhou HM Z (2013) Progress in enzyme immobilization in ordered mesoporous materials and related applications. Chem Soc Rev 42:3894–3912. https://doi.org/10.1039/c3cs60059a